JOURNAL OF MATERIALS SCIENCE **38** (2003) 4713–4723

Microindentation hardness of SB-block copolymers relating to nano-mechanical mechanisms

G. H. MICHLER*
Department of Engineering, Institute of Materials Science, Martin-Luther-Universität Halle-Wittenberg, D-06099 Halle/Saale, Germany
E-mail: michler@iw.uni-halle.de

F. J. BALTÁ-CALLEJA
Department of Macromolecular Physics, Instituto de Estructura de la Materia, CSIC, Serrano 119, 28006 Madrid, Spain

R. ADHIKARI
Department of Engineering, Institute of Materials Science, Martin-Luther-Universität Halle-Wittenberg, D-06099 Halle/Saale, Germany

K. KNOLL
BASF Aktiengesellschaft, Polymers Laboratory ZKT/I-B1, D-67056 Ludwigshafen, Germany

Asymmetric styrene/butadiene block copolymers and their blends with polystyrene homopolymer are studied, using transmission electron microscopy and scanning force microscopy, to explore the influence of phase morphology on the microindentation hardness and the nano-mechanical deformation mechanisms. In contrast to polymer blends and random copolymers, in which microhardness generally follows the additivity law, the behaviour of the investigated block copolymer systems is found to significantly deviate from the hardness additivity behaviour. Owing to the modified architecture, the asymmetric star block copolymer having 74 vol% polystyrene possesses a lamellar morphology, which partly explains the observed low hardness values. An additional explanation is found in the large plastic homogeneous deformation of the polystyrene (PS) lamellae by means of a new micromechanical mechanism called *thin layer yielding*. In the blends of a star block copolymer with polystyrene homopolymer, a rapid change in the micromechanical deformation behaviour is found to cause a shift in the observed microhardness to larger values. A major conclusion of our investigations is that microhardness of the triblock and star block copolymers can only be explained in the light of the morphology and nano-mechanical deformation mechanisms involved.

1. Introduction

Block copolymers form a new class of materials with unexpected and outstanding mechanical (stiffness, strength, toughness, etc.) and optical (transparency) properties. Amorphous block copolymers consisting of polystyrene (PS) and polyisoprene (PI) or polybutadiene (PB) units are examples of nanostructured heterogeneous polymers in which the mechanical properties are generally controlled by a microphase separated morphology that is adjustable by the block copolymer composition [1]. Through variation of molecular weight, composition, chain architecture and processsing conditions, the dimensions, nature and orientation of these structures can be accurately controlled [2]. In particular, the morphology of block copolymers having asymmetric chain architecture can markedly deviate from the classical phase diagram of diblock copolymers [3–8]. This allows one to prepare transparent nanostructured materials having a tailored mechanical property profile [6–9].

Poly(styrene-block-butadiene-block-styrene) (SBS) triblock copolymers, owing to the widely separated glass transition temperature (T_g) of the constituent phases, provide a broad range of service temperatures [1]. Their significance concerning technical applications lies in the fact that, at room temperature, the flexible rubbery polybutadiene blocks ($T_g \sim -100°C$) are anchored on both sides by the glassy polystyrene blocks ($T_g \sim +100°C$). Therefore, these block copolymers behave as a cross-linked rubber at ambient

* Author to whom all correspondence should be addressed.

temperature and allow a thermoplastic processing at higher temperature [2].

Because of the higher production costs involved, block copolymers are seldom used as pure materials. For example, styrene/butadiene block copolymers are often employed in combination with the polystyrene homopolymer (hPS) [2, 6]. Modification of the styrene/butadiene block copolymers' architecture does not only alter their phase diagram but also may change the degree of miscibility as well as the mechanical behaviour of their blends with polystyrene. One example of the latter are the block copolymers having an asymmetric star architecture. Indeed, as compared to their linear counterparts having analogous chemical composition and morphology, these star block copolymers are known to possess more attractive mechanical and rheological properties [6, 8, 9].

Owing to the wide interest in these block copolymers, a better understanding of their mechanical properties and a deeper insight into the structure-property-correlations is required. A bridge between the microphase structure or morphology and the mechanical properties are the micromechanical processes of deformation and fracture. Direct information on the micromechanical mechanisms can be gained using electron and scanning force microscopy techniques, including *in-situ* microscopy. These techniques permit a direct visualization of the morphology and its influence on the micromechanical deformation processes under the action of an applied load [10–12]. With help of these techniques we have characterized in detail the micromechanical properties of different amorphous [13, 14], semicrystalline [15, 16], rubber-toughened [17–22], particle-filled polymers [19] and block copolymers [23, 24].

Additional information can be gained from microhardness measurements. The microindentation hardness technique has found in recent years widespread application in polymer research [25]. The technique has been increasingly used in the characterization of homopolymers, polymer blends and copolymers. A very attractive feature of this technique is its ability for the micromechanical characterization of the polymeric materials. The influence of different molecular parameters (molecular weight, branching degree etc.) on the crystalline morphology in semicrystalline polymers, on the glass transition temperature in amorphous polymers [26–29] and the microphase separated morphology in block copolymers has been examined in preceding studies using the microhardness technique [30–32]. In particular, the microhardness behaviour of triblock and star block copolymers, binary block copolymer blends and blends containing homopolystyrene has been the object of recent studies [30–32]. The relevant finding here is that microhardness is not determined by the phase constitution of the block copolymers but mainly by the arrangement of the components, i.e., by the morphology. However, morphology changes alone could not satisfactorily explain the strong, unexpected deviation of the microhardness values from the additivity law. Therefore, it was concluded that additional contributions on the basis of new micromechanical mechanisms are necessary to clarify the new findings. The object of the present paper is, thus, to correlate the results obtained from microindentation hardness measurements with the micromechanical properties derived from direct microscopic observations, aiming to a better understanding of the plastic nano-mechanical processes occurring during microindentation in styrene/butadiene block copolymers.

2. Experimental

2.1. Materials and sample preparation

The characteristic data of the investigated block copolymers and of homopolystyrene are listed in Table I. The block copolymers possess an identical net chemical composition (styrene volume fraction = 0.74) but differ in the chain architecture. These copolymers were synthesised by the *sec*-butyl lithium initiated sequential living anionic polymerisation. To obtain asymmetric block copolymers (i.e., those having the styrene terminal blocks of unequal lengths), a different amount of styrene monomer was polymerised as the first and the last blocks of the chain. The tapered transition was achieved by allowing a mixture of styrene and butadiene monomers to simultaneously polymerise. Asymmetric star block copolymers were obtained by allowing the living linear chains of different lengths to couple via oligofunctional coupling agents. Further information about the synthesis of the block copolymer types used in the present study may be found elsewhere [6]. Their phase behaviour and morphology have been discussed in detail in preceding publications [6–8]. The star-block copolymer ST2 was used to prepare blends with general-purpose polystyrene homopolymer (hPS) by mixing the components in an extruder. The composition, PS content, thickness of the PS lamellae, D_{PS}, microhardness, H, elastic modulus, E, and yield stress, σ_y of these blends are collected in Table II. The materials investigated were prepared by injection moulding according to ISO 527 (mass temperature 250° and mould temperature 45°C) and solution casting using toluene as solvent.

2.2. Techniques

Tensile Testing was performed at room temperature (23°C) using a universal tensile machine (Zwick 1425)

TABLE I Characteristic data of the block copolymers and hPS studied

Sample	M_n (g/mol)[a]	M_w/M_n[a]	Φ_{ST}[b] (%)	Remarks
LN1-S74	82,000	1.07	74	SBS triblock with symmetric end blocks
ST2-S74	109,200	1.69	74	Highly asymmetric tapered star block with SB arm structure, PB core
hPS	82,600	2.30	100	Polystyrene homopolymer

[a]Determined by gel permeation chromatography (GPC) using PS calibration.
[b]Total styrene volume fraction determined by Wijs double bond titration.

TABLE II Composition, total PS content, thickness of the PS lamellae D_{PS}, microhardness H, Young's modulus E and yield stress σ_y of the ST 2/hPS blends

Sample	hPS content (wt%)	Total PS (wt%)	D_{PS} (nm)	H (MPa)	E (MPa)	σ_Y (MPa)
ST2	100	74	19	44	1205	24
ST2 + 20% hPS	80	79	27	64	1596	30
ST2 + 40% hPS	60	84	30	75	2072	37
ST2 + 60% hPS	40	90	39	100	2522	45
hPS	0	100	–	180	3300	55

at a cross head speed of 50 mm/min. At least 10 samples were tested in each case. The Young's modulus (E) and yield stress (σ_y) were calculated by evaluation of the initial slope and from the first maximum of the corresponding stress-strain curves, respectively.

Transmission electron microscopy (200 kV TEM, Jeol) was used to image the microphase separated morphology of the samples. Ultrathin sections (about 50–70 nm thick) were cut in a cryo-ultramicrotome from the bulk specimens. The polybutadiene phase was selectively stained by osmium tetroxide (OsO_4) vapour. The structures were characterised using a special image-processing program.

Microindentaion hardness (H) was evaluated by measuring the residual impression produced by a Vickers diamond indenter onto the surface of the injection moulded bars. For the sake of comparison, the indentations were made on the specimen surface in the middle of the injection moulded bars. An indentation time of 6 s and a load of 50 g were respectively used. The Vickers hardness is defined as [25]:

$$H = kP/d^2 \tag{1}$$

where P is the applied load in N, d the diagonal of the impression in m, and k a geometric factor equal to 1.854. The H values were derived from an average of at least 10 indentations.

Micromechanical characterization using TEM and SFM [10–12]:

(a) After deformation of the bulk material the deformed zones were stained using OsO_4 followed by preparing ultra-thin (about 100 nm) and semithin (about 500 nm thick) sections using a cryo-ultramicrotome. The sections were studied in a 200 kV TEM (Jeol) or a 1000 kV high voltage TEM (Jeol, in cooperation with the Max Planck Institute of Microstructure Physics in Halle/S.).

(b) Semithin sections (approximately 500 nm thick) were prepared from the bulk sample using a cryo-ultramicrotome and transferred to a special straining device that can be directly fitted to a microscope sample holder. Deformation of the samples was performed outside or inside the HVEM or a scanning force microscope (SFM). To improve the visibility of the polybutadiene phase in the deformed samples in the HVEM, an OsO_4 staining treatment of the strained samples was employed. In addition, the ultramicrotomed face of a bulk sample was investigated by tapping mode SFM using the phase imaging technique.

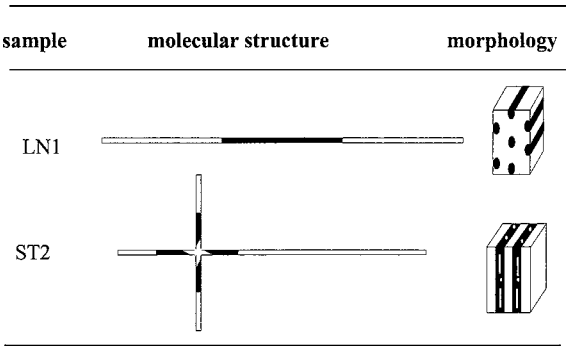

Figure 1 Schematics of molecular structure and morphology of the block copolymers studied (White and dark areas stand for hard (PS) and soft (PB) phases, respectively).

3. Molecular architecture and characterisation of morphology

In preceding studies we analysed the microphase-separated structure of the block copolymers investigated, using scanning force microscopy (SFM) and transmission electron microscopy (TEM) [7, 8]. The molecular architecture and morphology of the samples as revealed by the microscopic techniques are schematically represented in Fig. 1. Despite having the same chemical composition (74 vol% polystyrene), these block copolymers possess different morphologies as a consequence of modified molecular architecture of ST2.

The sample LN1 has a simple symmetric linear architecture (symmetric outer polystyrene blocks) held apart by a pure butadiene block having a sharp interface with the neighbouring polystyrene blocks. This sample displays morphology of hexagonal PB cylinders dispersed in the PS matrix, in agreement with the classical picture from the morphology of block copolymers (see Fig. 2a) [2].

The star-block copolymer ST2, having a highly asymmetric architecture and star topology, shows a lamellae-like 'two-component three-phase' morphology of alternating PS and PB lamellae (see Fig. 2b) [33]. The asymmetric structure as well as the presence of tapered interface allows a part of stiff polystyrene segments to be partially mixed to the polybutadiene phase suggesting a deviation of the apparent phase volume fraction from the actual phase ratio of the components. The influence of the modified architecture of the block copolymers additionally induces a shift of the glass transition temperature of the butadiene phase ($T_{g\text{-PB}}$) towards higher temperatures. For the sample LN 1, the values of T_g for polystyrene ($T_{g\text{-PS}}$) and polybutadiene ($T_{g\text{-PB}}$) blocks are about $+97^\circ$C and -95°C, respectively; i.e., they nearly correspond to the

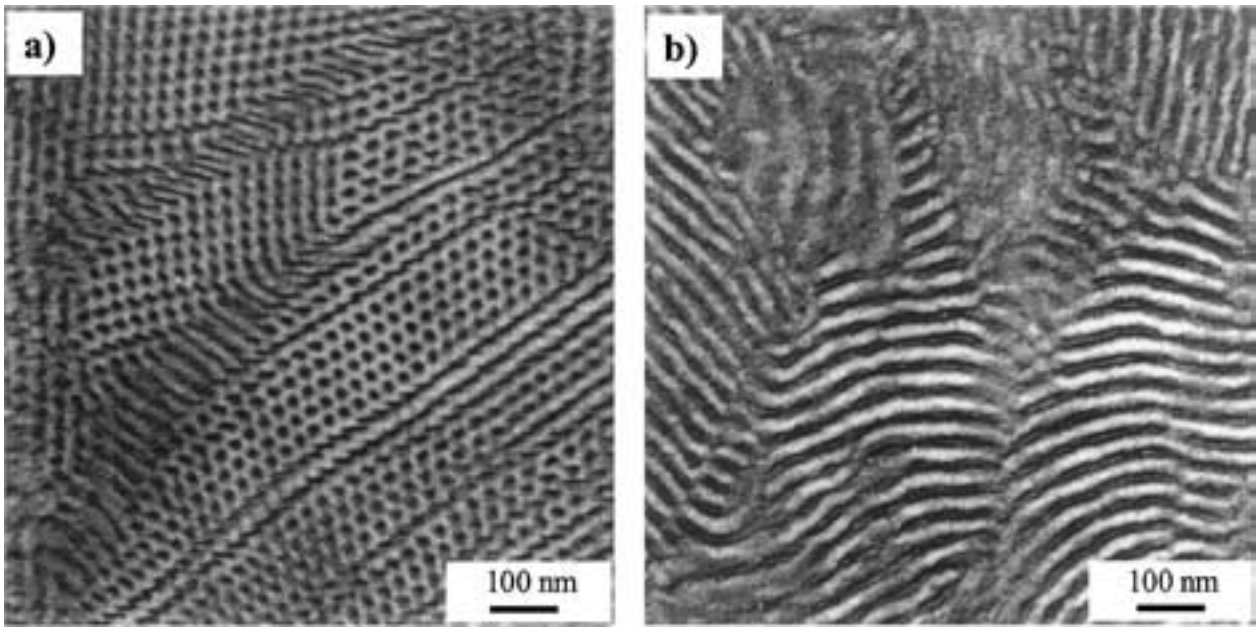

Figure 2 TEM micrographs showing the morphology of the block copolymers studied: (a) linear block copolymer LN1, and (b) star block copolymer ST2; solution cast films, OsO_4 staining.

glass transition temperatures of the corresponding homopolymers. However, the measured $T_{g\text{-PB}}$ value for the star block copolymer ST2 ($T_g = -79°C$) is much higher than that of PB homopolymer. This $T_{g\text{-PB}}$ increase is indicative of the presence of styrene units within the butadiene phase, which hinder the mobility of the flexible PB chains. In contrast to this, the $T_{g\text{-PS}}$ values of the samples remain nearly unchanged relative to that of PS homopolymer [33].

The lamellar morphology of the star block copolymer ST2 and the blends with hPS (see the TEM micrograph in Fig. 3) were oriented along the flow direction by injection moulding. It is worth mentioning that the morphology of the injection-moulded samples may change along the length of the bar and across the thickness of the sample. Therefore, for comparison purposes, the sections for the TEM studies were prepared from the middle of the injection moulded bar parallel to the injection direction at about 50 μm beneath the surface. By adding the hPS to the star block copolymer the morphology is continuously changed. Fig. 3 illustrates some representative TEM micrographs; the corresponding frequency distributions of the PS lamellae in the star block copolymer and the blends with hPS are presented in Fig. 4. It is to be noted that, both, the peak-maximum and the peak-width of the thickness distribution of the PS lamellae in the blends continuously shift towards higher values with increasing hPS content, indicating that a major part of the added hPS is accommodated into the corresponding PS lamellae of the star block copolymer. The thickness of the butadiene layers remains almost unchanged.

4. Results

4.1. Mechanical properties

The stress-strain curves of the block copolymers and some of the ST2/hPS blends are presented in Fig. 5a and b. According to these curves three types of mechanical behaviour can be identified for these materials:

(a) Sample LN1 with a relatively high stiffness (elastic modulus), high yield stress, and low elongation at break and, therefore, showing a low toughness
(b) Sample ST2 presenting a remarkably large elongation at break and, consequently, a high ductility (toughness)
(c) The blends of ST2 revealing a decreasing elongation at break with increasing hPS content.

4.2. Microhardness measurements

Fig. 6 shows the plot of microhardness as a function of total styrene content for the block copolymers and blends. The dotted straight line illustrates the hardness as a function of composition according to the additivity law (Equation 2):

$$H = H_{PS} \cdot \Phi_{PS} + H_{PB} \cdot (1 - \Phi_{PS}) \qquad (2)$$

where H_x and Φ_x represent the microhardness and the weight fraction of the component X, respectively. The obtained results reveal a conspicuous deviation of H-data from the additivity law and display a relatively wide range of H-values in spite of having an identical net chemical composition in case of the pure block copolymers. Similarly to the mechanical properties (see Fig. 5) one can distinguish three different H-ranges depending on the microphase-separated morphology type:

(a) Sample LN1 showing a hardness of $H = 72$ MPa.
(b) Sample ST2 presenting a lower hardness value of $H = 45$ MPa.
(c) The blends of ST2 that show increasing hardness values in the range 64–100 MPa. with increasing hPS content

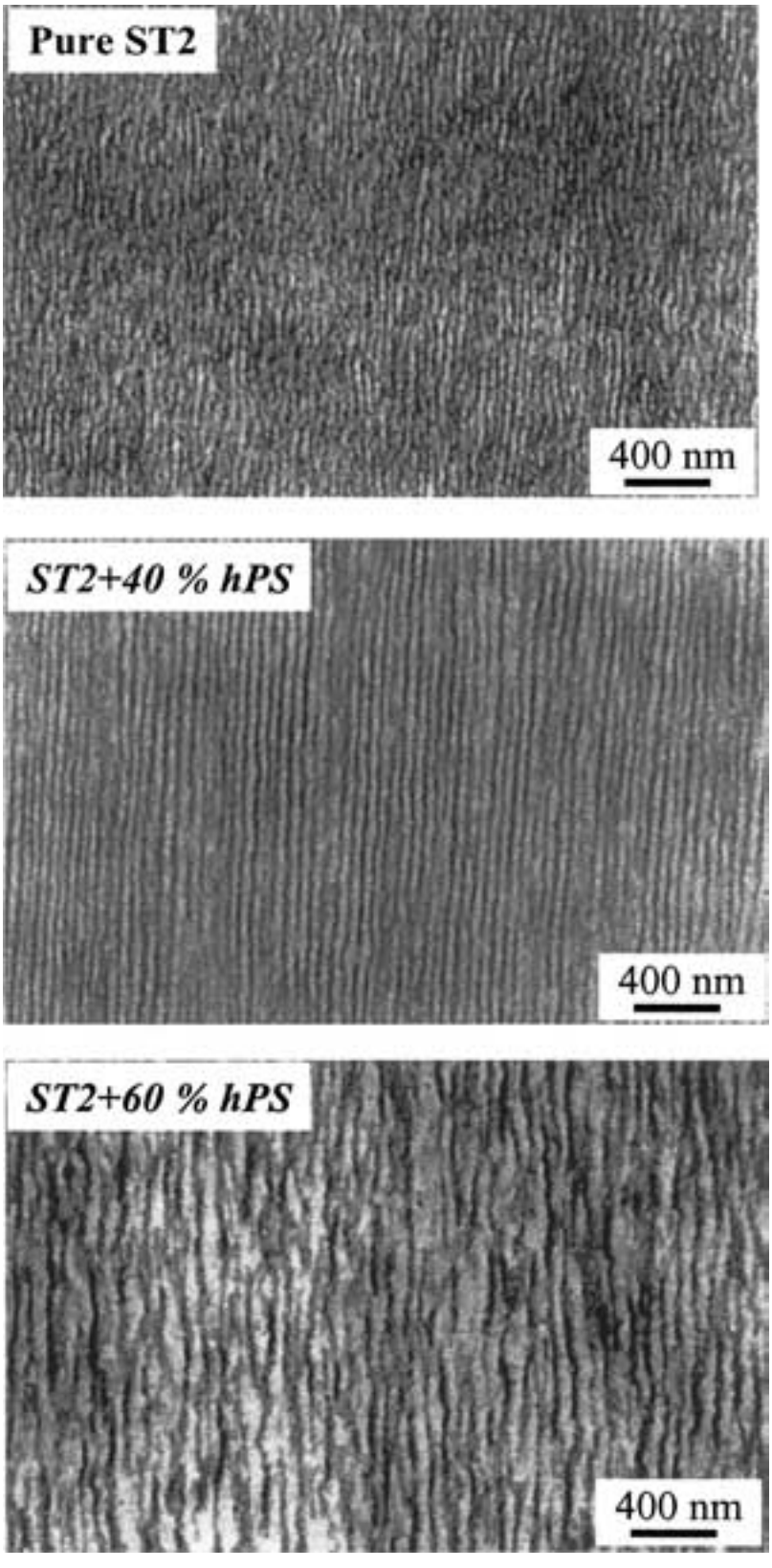

Figure 3 TEM micrographs of the injection-moulded star block copolymer and of the blends with hPS for two compositions.

It should be noted that the H values of the block copolymers show a decrease with increasing $T_{g\text{-}PB}$. As discussed above, the $T_{g\text{-}PB}$ increase points to the presence of styrene units in the butadiene phase, contributing to an increase of total soft phase volume fraction. However, since the $T_{g\text{-}PB}$ value is much lower than test temperature, the hardness of the soft phase can be assumed to be negligible (following the additivity law), i.e., the variation of $T_{g\text{-}PB}$ should not have any influence on the hardness of the copolymers (for further details see [30]). The reason for the low hardness values obtained and the deviations from the additivity law has to be looked- for not only in the morphology but also, most specially, in the micromechanical behaviour under the indenter, as it will be discussed below.

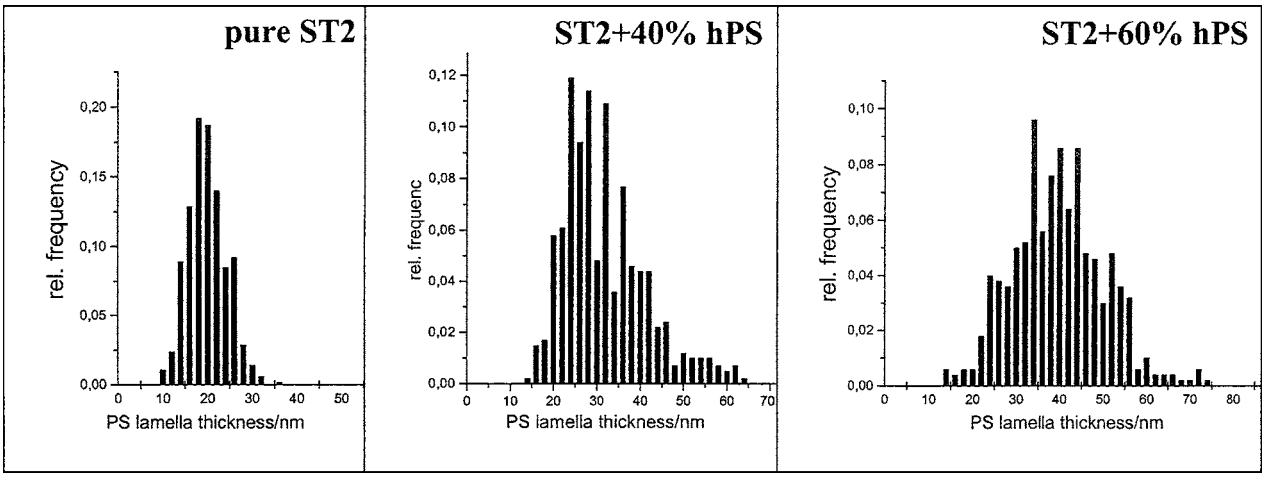

Figure 4 Thickness distribution of PS lamellae for the samples having the morphologies shown in Fig. 3.

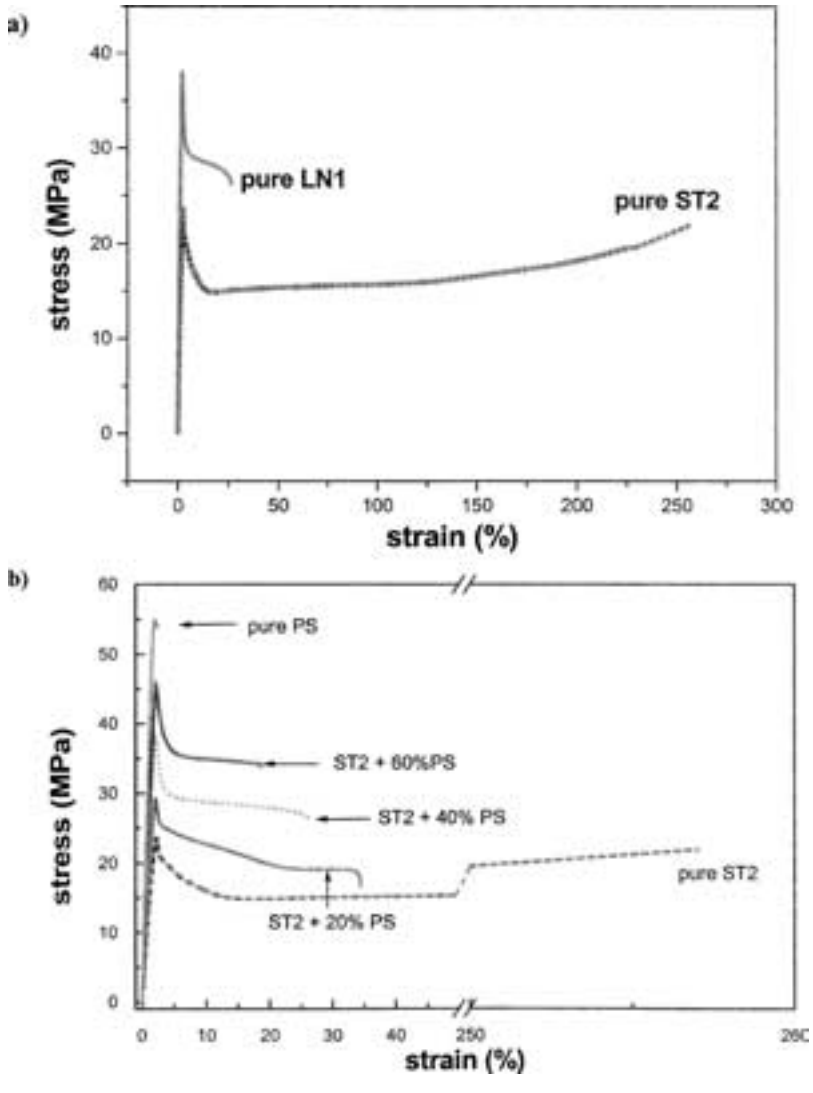

Figure 5 Stress-strain curves of the samples investigated: (a) pure block copolymers, and (b) ST2/hPS blends.

4.3. Nano-mechanical processes and mechanisms

The deformation processes occurring in the samples during mechanical loading can be clearly observed in the micrographs taken from deformed zones of the samples. Three types of micromechanical behaviour can again be distinguished:

(a) In case of sample LN1 (morphology of the PS matrix with PB cylinders), PS-matrix strands between the PB cylinders are cavitated and fibrillated, forming together with elongated PB cylinders craze-like deformed structures (see Fig. 7).

(b) In case of ST2 (lamellar morphology) (see Fig. 8a); if the deformation direction is parallel to the

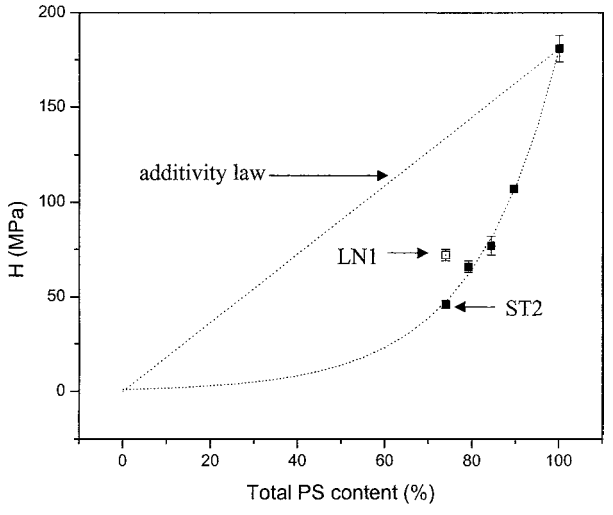

Figure 6 Plot of microhardness of the block copolymers and blends as a function of total PS-content. The dotted straight line represents the calculated hardness versus composition according to the additivity law.

lamellar orientation, a homogeneous plastic yielding of, both, PS and PB lamellae is detectable (Fig. 8b). Apparently there is no change in the phase morphology besides a significant variation of the layer thicknesses and long period. However, a clear reduction of the PS lamellae-thickness after deformation is observed (compare Fig. 8a and b). This mechanism of homogeneous plastic deformation, called *thin layer yielding* is quite different from the usual (craze-like) behaviour of polystyrene [8].

If the deformation direction is perpendicular or oblique to the lamellar orientation, different mechanisms may act simultaneously or one after another (see Fig. 9). First, a shift of adjacent lamellae (gliding process) occurs. Thereafter, the lamellae break into smaller domains, rotating towards the loading direction. Finally, chevron-like or fir-tree like morphologies are formed (Fig. 9).

(c) In case of blends of ST2 with different amount of hPS,: when the applied deformation is parallel to the direction of the lamellar orientation a transition appears, with increasing thicker PS lamellae, from the thin layer yielding mechanism to a crazing mechanism (see Fig. 10). The internal structure of the crazes consists of cavitated and extended PS lamellae and elongated PB lamellae. With increasing PS content, there is a parallel increase of Young's modulus E and yield stress σ_y (see Table II).

5. Discussion

5.1. Microhardness and morphology

A deviation of the hardness values from the additivity law has been shown to occur in other polymers, e.g., in rubber modified semicrystalline polymers (iPP), in which the hardness of the crystals within the blends is lower than in the homopolymer [34]. However, the deviation in the H-values observed in the present study is significantly larger than that observed in other polymer materials. The larger deviations detected here suggest that the total styrene content present in the block copolymers and in the blends containing hPS bears no correlation with the microhardness data. Instead, the nature of the microphase- separated morphology appears to play a relevant role. In ST2, the change in the phase morphology and the parallel increase of the glass transition temperature of the soft phase ($T_{g\text{-PB}}$) give rise to a partial incorporation of PS molecules into the PB phase. Consequently, a rise of the apparent soft phase volume and a parallel change of

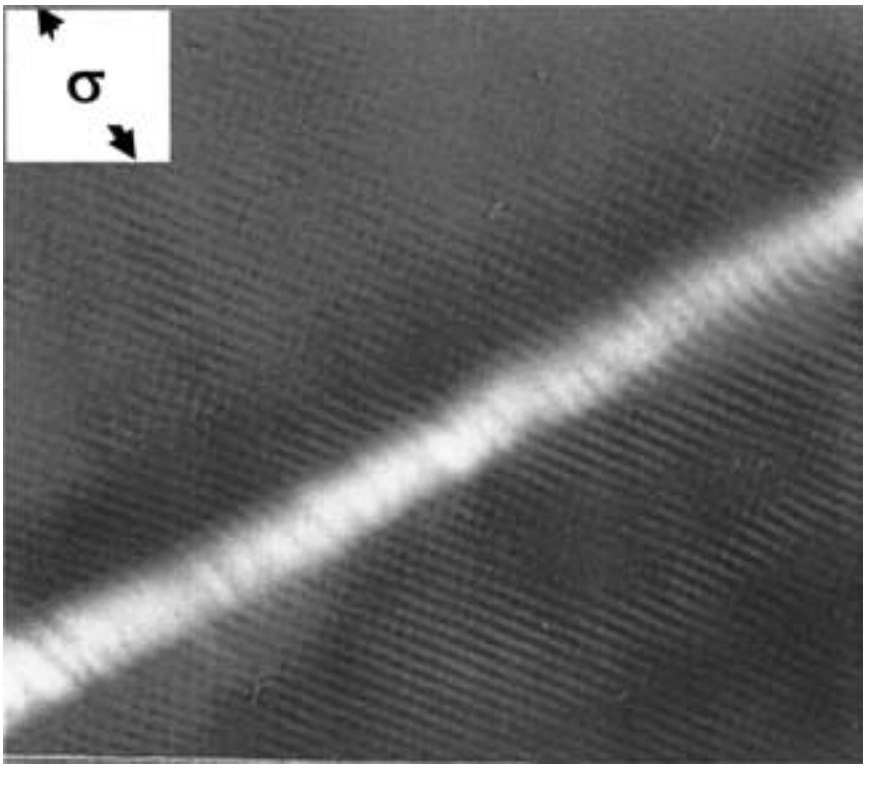

Figure 7 TEM micrograph showing craze-like deformation bands in the block copolymer LN1.

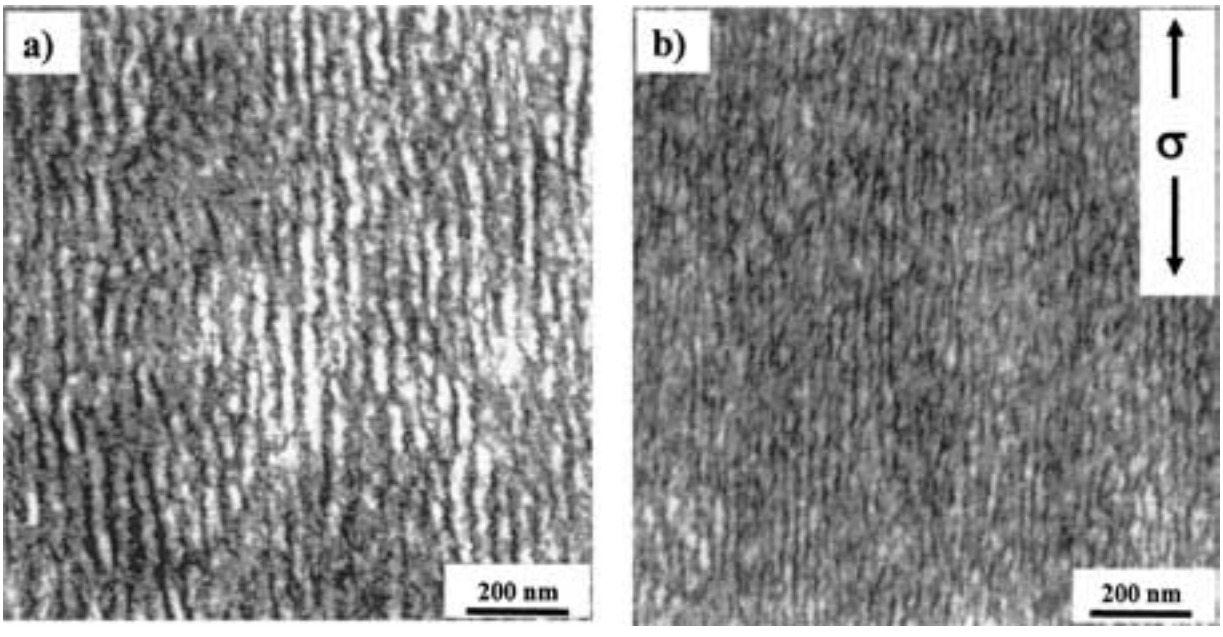

Figure 8 Lamellar block copolymer: (a) undeformed and (b) after deformation parallel to the lamellar orientation via homogeneous yielding of PS and PB lamellae (mechanism of *thin layer yielding*).

PB domains or cylinders into PB lamellae might take place leading, as a result, to the observed hardness decrease.

By adding hPS to the block copolymers the hardness-value increase rather abruptly. Since no parallel changes in the morphology are observed, the explanation for this sudden increase has to be found in the micromechanical processes occurring below the indenter (see next section).

5.2. Microhardness and micromechanical processes

The block copolymer sample ST2 with a lamellar morphology exhibits the lowest hardness values. In this sample, the mechanisms of *thin layer yielding* or formation of *chevron-like* morphology (depending on the direction of deformation relative to the lamellar orientation) take place. These mechanisms are sketched in Fig. 11. Here, the starting processes are connected with the high mobility and easy deformability of the soft PB phase. This could be clearly shown by analysing the strain induced molecular orientation of individual phases by means of Fourier transform infrared (FTIR) spectroscopy [33, 35]. The latter reveals a molecular orientation mainly in the PB phase in the initial stages of deformation. Up to about 50% strain the orientation of the PB chains parallel to the deformation direction increases remarkably. On the other hand, the PS chains only show a very small

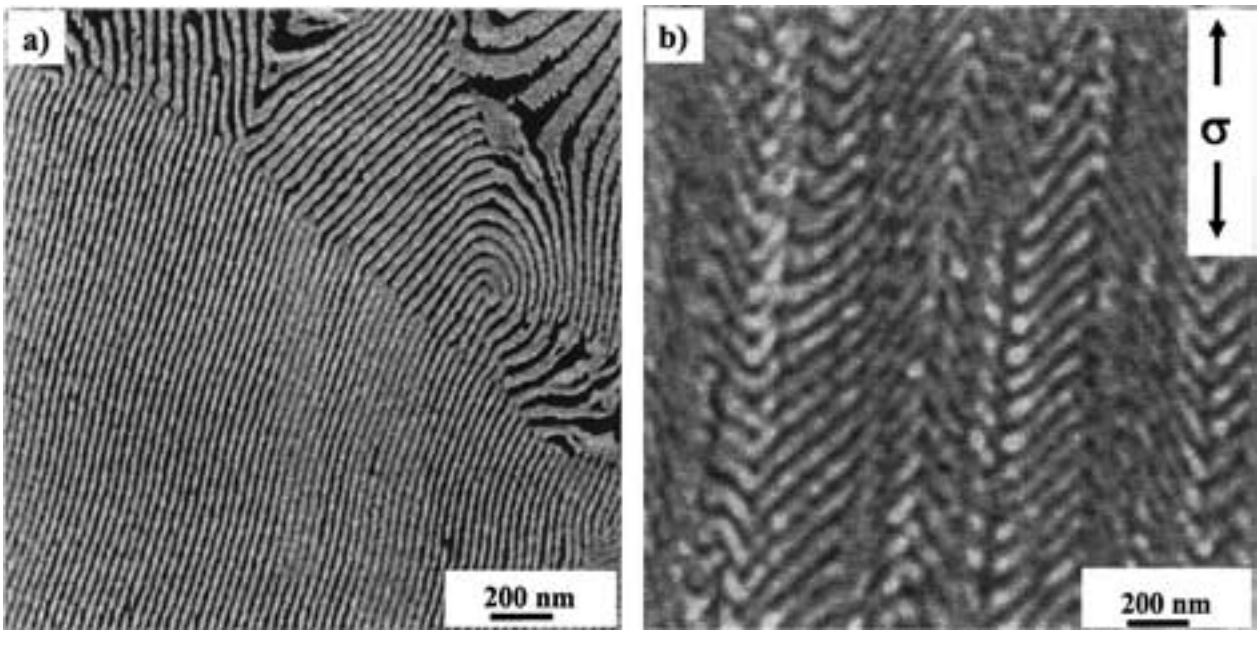

Figure 9 Lamellar block copolymer: (a) undeformed and (b) after deformation perpendicular to the lamellar orientation direction with the processes of lamellae shifting and twisting (mechanism of *chevron formation*).

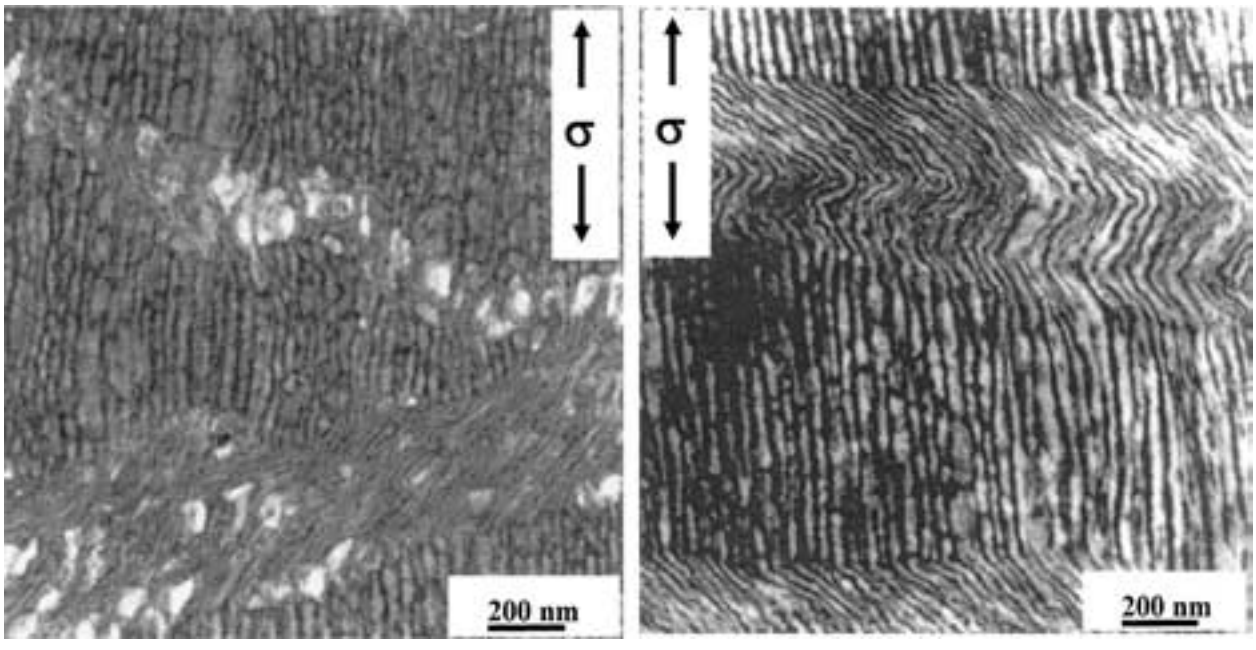

Figure 10 Deformation of ST2 blends with hPS in the parallel direction to the orientation of PS lamellae: formation of fibrillated crazes: (a) 20 wt% hPS, and (b) 40 wt% hPS.

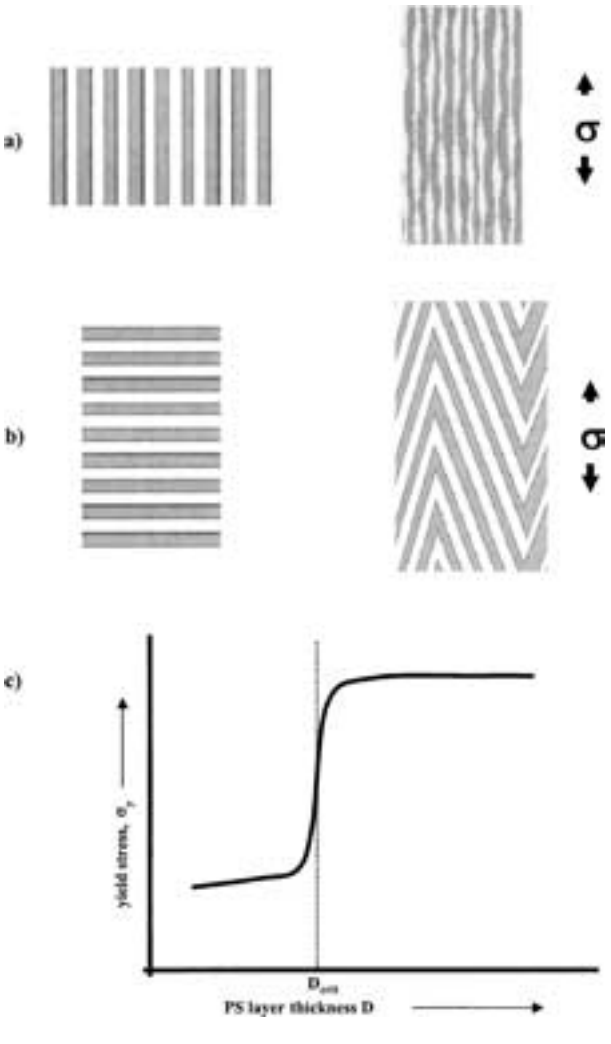

Figure 11 Schematics of deformation mechanisms for the lamellar block copolymers: (a) deformation parallel to the lamellar orientation (*thin layer yielding mechanism)*, (b) deformation perpendicular to the lamellar orientation (*formation of chevron- or fir-tree like zones)*, and (c) yield stress of PS lamellae as a function of lamellae thickness *D*.

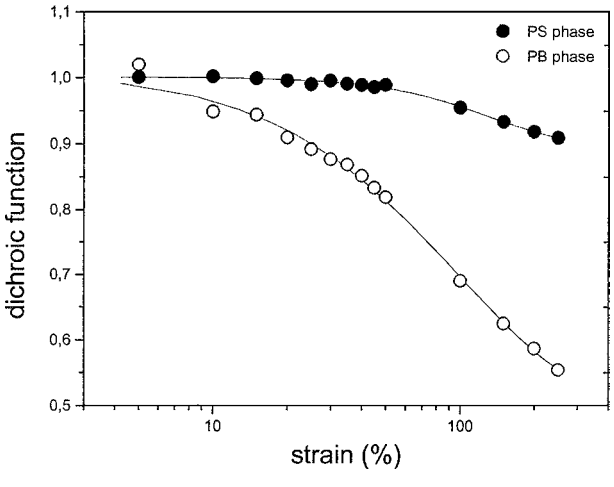

Figure 12 Dichroic function representing the molecular orientation of individual phases of the block copolymer ST2, derived from FTIR spectroscopy.

orientation—(see Fig. 12; details in [35]). Plastic deformation, thus, starts with the yielding process, including lamellae shifting, lamellar separation and twisting of PS lamellae, in other words, involving a plastic deformation in the soft phase and an alignment of lamellae parallel to the loading direction. For higher deformations, depending on the loading direction with respect to the lamellar orientation direction, a plastic deformation (yielding) of PS lamellae starts immediately. (Fig. 11a), or after breaking and twisting of PS lamellae with the formation of *chevron-like* bands (Fig. 11b). Here, the deformation of the PS lamellae reaches 200–300% with a corresponding orientation increase of the PS molecules [33, 35]. Accordingly, there is the following situation below the indenter as load increases:

At the beginning of indentation process (for small strains) the harder PS lamellae undergo a ‘slipping’

process, mainly due to the easy mobility of the PB phase up to deformations of about 50%. For larger strains, after shifting and twisting the lamellae, homogeneous plastic yielding of the PS lamellae (via *thin layer yielding* mechanism) occurs. Since the indentation depth (under the experimental conditions applied) is in the range of a few μm, we can assume that the deformation processes under the indenter predominantly take place in the soft phase though a beginning of yielding in the PS lamellae also occurs. Both yielding processes are connected to low yield-stresses leading to the very low hardness values observed.

In case of the blends with hPS, the thickness of the PS lamellae is increased to such an extent that the mechanism of 'thin layer yielding' does not take place anymore. Above a critical layer thickness of about 20–30 nm (at room temperature) [8] the PS lamellae turn from the ductile behaviour on a nanometer scale into the usual brittle behaviour of bulk PS. Therefore, the yield stress of the PS lamellae, and consequently of the whole material, is increased (see Table II and Fig. 11c), resulting in larger hardness values. The hardness increases more rapidly than expected from the PS content-increase according to the additivity law. Indeed, an addition of 60 wt% hPS to the star block copolymer ST2 results in a hardness increase by 56 MPa (from 44 to 100 MPa; see Table II) whereas with a total PS- increase of 16 vol% (from 74 to 90 vol%), the additivity law would give a hardness increase of only 30 MPa—(see Fig. 6).

6. Conclusions

The microhardness study of various styrene/butadiene block copolymers and blends containing hPS reveals values that are much lower than those expected from the hardness-additivity law. There are two reasons that may explain the deviation from the additivity behaviour:

(1) The occurrence of a morphology quite different from the expected one on the basis of the phase content in the materials. Owing to a partial mixing of PS molecules with the PB phase, the soft phase content is increased with a corresponding shift to a morphology of alternating PS and PB lamellae, giving rise to a higher glass transition temperature of the soft phase. The change in morphology with an apparently increased soft phase leads to the hardness decrease observed.

(2) The second reason lies in the occurrence of new micro- or nano-mechanical mechanisms, that enable an easier plastic deformability of the otherwise brittle PS. Owing to the *thin layer yielding* mechanism the material below the indenter can yield with a reduced yield stress.

Results show that in the block copolymer systems used, the microhardness is not determined by the amount of components (i.e., phase composition and additivity law), but mainly by the real morphology and new micromechanical effects on the nm-scale.

Acknowledgements

This project is funded by the Deutsche Forschungsgemeinschaft and by MCYT, Spain (grants BFM 2000-1474 and HA 2000-0070). Financial support from the Deutscher Akademischer Austauschdienst (DAAD) and from the Alexander von Humboldt-Stiftung are acknowledged. One of us (GHM) thanks the Dirección General de Universidades, Ministerio de Educatión, Spain, for the award of the Humboldt-Mutis Prize.

References

1. G. HOLDEN, "Understanding Thermoplastic Elastomers" (Carl Hanser, Munich, 2000).
2. I. W. HAMLEY, "The Physics of Block Copolymers" (Oxford Science Publishers, London, 1998).
3. S. T. MILNER, *Macromolecules* **27** (1994) 2333.
4. M. W. MATSEN, *J. Chem. Phys.* **113** (2002) 5539.
5. C. LEE, S. P. GIDO, Y. POULOS, N. HASDICHRISTIDIS, N. B. TAN, S. F. TREVINO and J. W. MAYS, *ibid.* **107** (1997) 6470.
6. K. KNOLL and N. NIESSNER, *Macromol. Symp.* **132** (1998) 231.
7. R. ADHIKARI, R. GODEHARDT, W. LEBEK, R. WEIDISCH, G. H. MICHLER and K. KNOLL, *J. Macromol. Sci.*, B **40** (2001) 833.
8. G. H. MICHLER, R. ADHIKARI, W. LEBEK, S. GOERLITZ, R. WEIDISCH and K. KNOLL, *J. Appl. Polym. Sci.* **85** (2002) 683.
9. J. S. SHIM and J. P. KENNEDY, *J. Polym. Sci.* A **38** (2000) 279.
10. G. H. MICHLER, "Kunststoff-Mikromechanik: Morphologie, Deformations-und Bruchmechanismen" (Carl Hanser, München,1992).
11. *Idem*., *Trends Polym. Sci.* **3** (1995) 124.
12. *Idem*., *J. Macromol. Sci.* B **38** (1999) 787.
13. *Idem*., *J. Matr. Sci.* **25** (1990) 2321.
14. *Idem*., in "Deformation and Fracture of Polymers," edited by W. Grellmann and S. Seidler (Springer, Berlin, 2001) p. 193.
15. *Idem*., *Coll. Polym. Sci*. **270** (1992) 627.
16. G. H. MICHLER and R. GODEHARDT, *Cryst. Res. Technol.* **35** (2000) 863.
17. G.-M. KIM, G. H. MICHLER, M. GAHLEITNER and J. FIEBIG, *J. Appl. Polm. Sci.* **60** (1996) 1391.
18. J.-U. STARKE, R. GODEHARDT, G. H. MICHLER and C. B. BUCKNALL, *J. Matr. Sci.* **32** (1997) 1855.
19. G.-M. KIM and G. H. MICHLER, *Polymer* **39** (1998) 5699; *ibid*. p. 5699.
20. G.-M. KIM, G. H. MICHLER, M. GAHLEITNER and R. MÜLHAUPT, *Polym. Adv. Technol.* **9** (1998) 709.
21. J. LAATSCH, G.-M. KIM, G. H. MICHLER, T. ARNDT and T. SÜFKE, *ibid.* **9** (1998) 716.
22. G. H. MICHLER and C. B. BUCKNALL, *Plast. Rub. Comp.* **30** (2001) 110.
23. R. WEIDISCH, M. ENßLEN, G. H. MICHLER and H. FISCHER, *Macromolecules* **32** (1999) 5375.
24. R. WEIDISCH and G. H. MICHLER, in "Block Copolymers," edited by F. J. Baltá-Calleja and Z. Roslaniec (Marcel Dekker, New York, 2000) p. 215.
25. F. J. BALTÁ-CALLEJA and S. FAKIROV, "Microhardness of Polymers" (Cambridge University Press, Cambridge, 2000).
26. *Idem*., in "Block Copolymers," edited by F. J. Baltá-Calleja and Z. Roslaniec (Marcel Dekker, New York, 2000) p. 179.
27. M. KRUMOVA, J. KARGER-KOCSIS, F. J. BALTÁ-CALLEJA and S. FAKIROV, *J. Mater. Sci.* **34** (1999) 2371.
28. S. FAKIROW, F. J. BALTÁ-CALLEJA and M. KRUMOVA, *J. Polym. Sci.* B **37** (1999) 1413.
29. F. J. BALTÁ-CALLEJA, E. G. PRIVALKO, A. M. FAINLEIB, T. A. SHANTALII and V. A. PRIVALKO, *J. Macromol. Sci.—Phys*. B **39** (2000) 131.

30. G. H. MICHLER, F. J. BALTÁ-CALLEJA, I. PUENTE, M. E. CAGIAO, K. KNOLL, S. HENNING and R. ADHIKARI, *J. Appl. Polym. Sci*., in press.
31. R. ADHIKARI, G. H. MICHLER, M. E. CAGIAO and F. J. BALTÁ-CALLEJA, *J. Polym. Eng.*, in press.
32. F. J. BALTÁ-CALLEJA, M. E.CAGIAO, R. ADHIKARI and G. H. MICHLER, *Polymer*, in press.
33. R. ADHIKARI, G. H. MICHLER, T. A. HUY, E. IVANKOVA, R. GODEHARDT, W. LEBEK and K. KNOLL, *Macromol. Chem. Phys.* **204** (2003) 488.
34. A. FLORES, F. J. BALTÁ-CALLEJA, J. AURREKOETXEA, R. GENSLER and H. H. KAUSCH, *Coll. Polym. Sci.* **276** (1998) 786.
35. T. A. HUY, R. ADHIKARI and G. H. MICHLER, *Polymer* **44** (2003) 1247.

Received 18 March
and accepted 1 July 2003